Mobilities of the Inner Three Core Residues and the Man(α1→6) Branch of the Glycan at Asn78 of the α-Subunit of Human Chorionic Gonadotropin Are Restricted by the Protein†

Carol W. E. M. Thijssen-van Zuylen,‡,§ Tonny de Beer,‡,|| Bas R. Leeflang,‡,⊥ Rolf Boelens,⊥ Robert Kaptein,⊥ Johannis P. Kamerling,‡ and Johannes F. G. Vliegenthart*,‡

Department of Bio-Organic Chemistry and Department of NMR Spectroscopy, Bijvoet Center, Utrecht University, Padualaan 8, 3584 CH, Utrecht, The Netherlands

Received July 30, 1997; Revised Manuscript Received November 10, 1997

ABSTRACT: Human chorionic gonadotropin (hCG) is a heterodimeric glycoprotein hormone involved in the maintenance of the corpus luteum in early pregnancy. The free α-subunit of hCG has a biological activity of its own, namely, stimulation of prolactin secretion from term pregnancy decidual cells [Blithe, D. L., et al. (1991) *Endocrinology 129*, 2257−2259]. Glycosylation at Asn78 of the α-subunit is required for the stability of the protein, but the exact nature of the stabilizing effect is not known. In our previous study, it was indicated that GlcNAc-**1** at Asn78 has a reduced mobility, whereas the glycan at Asn52 is highly mobile [De Beer, T., et al. (1996) *Eur. J. Biochem. 241*, 229−242]. In the present investigation, it is shown that the PNGase F susceptibility of the Asn52-linked glycan in the free α-subunit is absent in the heterodimer. Thus, the high mobility of the glycan at Asn52 may be characteristic for the free α-subunit. For accurate modeling of αhCG, knowledge of the behavior of each of the glycans is essential. In this context, the mobility of the glycans and their interactions with the protein are explored by NMR spectroscopy using desialylated, partially deglycosylated free α-subunit (as-pdα) carrying glycans at Asn78 only. NOEs between GlcNAc-**2** and several amino acid residues indicate that GlcNAc-**2** is involved in stabilizing αhCG. From the values of ^{13}C relaxation parameters T_2 and $T_{1\rho}$ of the constituting monosaccharide residues, it was concluded that the inner three residues have a severely restricted mobility. The Man-**4** and Man-**4′** residues of the diantennary oligosaccharide exhibit a similar relaxation behavior, suggesting that the Man-**4′** branch occurs in a single conformation of the C5−C6 linkage of Man-**3** instead of in rapidly interconverting conformations that are known to exist for this linkage for the free oligosaccharide.

Human chorionic gonadotropin (hCG[1]) is the placental member of the glycoprotein hormone family that further includes the pituitary hormones follitropin, lutropin, and thyrotropin. hCG exerts its activity through binding to a G-protein-coupled receptor in luteal cells resulting in increased adenylate cyclase activity. This is essential for the maintenance of the corpus luteum in early pregnancy (*1*−*3*). The hormone is a heterodimer consisting of two noncovalently associated glycosylated subunits, α and *β*. The α-subunit consists of 92 amino acids that are identical for all members of the hormone family. It is N-glycosylated at Asn52 and Asn78. Site-directed mutagenesis revealed that the glycan at Asn52 is essential for biological activity (*4*), whereas the glycan at Asn78 is involved in stabilizing the protein (*5*). The carbohydrate structures attached to Asn78 are mono- and diantennary *N*-acetyllactosamine type glycans in a ratio of 4:6 [(*6*), Figure 1].

Only a few studies have been carried out to determine the structure and conformation of the N-linked oligosaccharide part of intact glycoproteins in solution. Hen phosvitin has been subjected to NMR spectroscopy, and a high degree of similarity of chemical shifts and coupling patterns between the glycan part in the intact protein and model oligosaccharides was found, suggesting similar conformations (*7*). An extensive study on CD2 revealed that the Asn-linked GlcNAc residue stabilizes the protein structure by counterbalancing an unfavorable clustering of five positive charges (*8, 9*) and that only the resonances corresponding to GlcNAc-**1** and -**2** differ significantly from those of comparable free glycans. Also for CD58, only contacts between the Asn-linked

† This investigation was supported by The Netherlands Foundation for Chemical Research (SON) with financial aid from The Netherlands Organization for Scientific Research (NWO).

* Corresponding author.

‡ Department of Bio-Organic Chemistry.

§ Present address: Department of Analytical Chemistry for Research, N.V. Organon, P.O. Box 20, 5340 BH Oss, The Netherlands.

|| Present address: Department of Pharmacology, University of Colorado HSC, Box C236, 4200 East Ninth Avenue, Denver, CO 80262.

⊥ Department of NMR Spectroscopy.

[1] Abbreviations: (α)hCG, (α-subunit of) human chorionic gonadotropin; PNGase F, peptide-N^4-(*N*-acetyl-*β*-glucosaminyl)asparagine amidase F; sialidase, acylneuraminyl hydrolase; as-pdα, αhCG desialylated and site-specifically deglycosylated at Asn52, sialidase, and PNGase F-treated native αhCG; MLEV, composite spin-lock pulse devised by M. Levitt; ROE, rotating-frame nuclear Overhauser enhancement; TPPI, time-proportional phase increment; INEPT, insensitive nuclei enhanced by polarization transfer; HSQC, ^1H-detected heteronuclear single-quantum coherence spectroscopy.

S0006-2960(97)01854-0 CCC: $15.00
Published on Web 01/30/1998

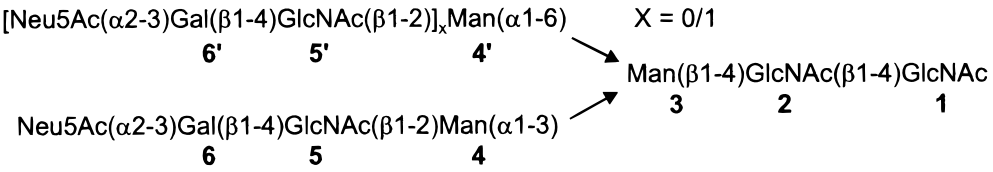

FIGURE 1: Glycans attached to Asn78 of the α-subunit of human chorionic gonadotropin.

GlcNAc and the protein were found (*10*). The mobility of the oligosaccharide part of intact glycoproteins has not been the subject of many studies as yet. ^{13}C relaxation measurements were reported on ribonuclease B (*11*), and a study using molecular dynamics simulations and NOESY analysis was performed on bromelain (*12, 13*). In the latter study, a model was developed to estimate characteristic times for large reorientations around the glycosidic linkages associated with conformational transitions.

In the present study, the mobility of a glycan as a part of an intact glycoprotein was studied directly using NMR relaxation measurements. In the framework of our previous investigations of hCG, almost all chemical shifts of αhCG were assigned. Also, the broadening beyond detection of signals in heteronuclear NMR spectra for the Asn78-linked GlcNAc residue indicated a restricted mobility (*14, 15*). NMR spectroscopy was applied to analyze the oligosaccharide moiety of desialylated, partially deglycosylated αhCG (as-pdα) carrying the glycan at Asn78 only. It was investigated how glycosylation at Asn78 stabilizes the structure of αhCG. Furthermore, ^{13}C relaxation studies were carried out to determine the extent to which the flexibility of this glycan is affected by the protein.

EXPERIMENTAL PROCEDURES

Sample Preparation. αhCG or hCG (125 μg) was dissolved in 100 mM NaAc buffer, pH 5.7, containing 10 mM EDTA and 10 mM NaN_3. Samples were incubated with or without 0.17 U of peptide-N^4-(*N*-acetyl-β-glucosaminyl)-asparagine amidase F (PNGase F) for 16 h at 37 °C, in a final volume of 50 μL, and aliquots containing 2.5 μg of protein were applied on a 15% SDS−polyacrylamide gel.

For the preparation of the NMR sample, purification of αhCG from an acetone precipitate of urine from pregnant women and removal of terminal sialic acid were performed as described before (*16*). Following desialylation, NaN_3 and EDTA were added to the mixture up to concentrations of 1 and 30 mM, respectively. Then, the reaction mixture (final volume 8.2 mL) was incubated with 150 U of PNGase F for 16 h at 37 °C. Protein and released glycans were separated and desalted using gel filtration as described (*16*). Protein samples were dissolved in ^1H_2O or ^2H_2O, containing 0.1 M NaCl. To the ^1H_2O sample, NaN_3 was added to 1 mM. The pH was adjusted to 5.1 (^1H_2O) or 4.7 (^2H_2O) (pH meter reading was not corrected for the ^2H-isotope effect). αhCG and as-pdα concentrations were 5 mM, as determined by absorbance at 280 nm with a molar absorption coefficient of 6.4×10^3 M^{-1} cm^{-1} (*17*).

NMR Spectroscopy. NMR spectra were recorded at 328 or 338K on Bruker AMX 500, Bruker AMX 600, or Varian Unity Plus 750 MHz spectrometers (Bijvoet Center, Utrecht University and NSR Center, University of Nijmegen). In all experiments the water resonance was suppressed by low-power presaturation during the relaxation delay. In addition, during NOE mixing times, low-power irradiation of ^1H_2O was applied and in spectra recorded on Bruker spectrometers, also a homo-spoil pulse of 5 ms was applied along the *z*-axis, followed by a recovery delay of 15 ms. The TOCSY spectrum at the 750 MHz spectrometer was recorded with a pulse sequence for a 3D NOESY−TOCSY (*18*) where the t_1 evolution period of the 3D experiment was kept constant. For all spectra recorded at the Varian 750 MHz spectrometer, a pulsed-field gradient (sine-bell, 1 ms, 0.3 mT/cm) was applied during the relaxation delay to remove any nonrelaxed signals.

A two-dimensional double-quantum filtered COSY spectrum was recorded as described (*19, 20*). Two-dimensional TOCSY spectra (*21*) were recorded with mixing times of 40−70 ms by means of an MLEV-17 spin-lock pulse sequence (*22, 23*) preceded by a 2.5 ms trim pulse. Two-dimensional ^1H−NOE spectra (*24*) were recorded with mixing times of 50−80 ms. A two-dimensional ^1H rotating-frame nuclear Overhauser enhancement (ROE) spectrum (*25*) was recorded with mixing times of 50−150 ms as described previously (*15*). Gradient-enhanced two-dimensional (^1H−^{13}C) ^1H-detected heteronuclear single-quantum coherence (HSQC) spectra (*26*) with pulsed field gradients to suppress artifacts and to reduce the need for phase cycling (*27*) were recorded as described (*14*).

Relaxation delays were between 700 and 850 ms, and two-dimensional ^1H NMR spectra were recorded with 512−600 t_1 experiments. For the HSQC spectra per experiment 160 or 112, free induction decays of 2048 complex data points were collected, and spectral widths were 6024 or 5747 Hz in the t_2 dimension and 21741 or 11318 Hz in the t_1 dimension for αhCG or as-pdα, respectively. For the as-pdα spectrum, the ^{13}C carrier frequency was placed at 77.5 ppm, and 750 experiments were recorded in the t_1 dimension. To achieve quadrature detection in the indirectly detected dimensions, either time-proportional phase incrementation [TPPI (*28*)] or the States-TPPI method (*29*) was used.

Line Width and $T_{1\rho}$ Experiments. The HSQC spectra recorded for the determination of line widths and $T_{1\rho}$ values were extended by a pulse scheme for sensitivity enhancement (*30, 31*). Experiments were optimized to have the highest resolution and signal/noise ratio in the anomeric region by placing the carrier frequency at 103.5 ppm and reducing the sweep width in the t_1 dimension to 2716 Hz. The pulse sequence for the two-dimensional sensitivity- and gradient-enhanced natural abundance ^{13}C $T_{1\rho}$ relaxation measurements is presented in Figure 2 (*32*). Two sets of seven spectra with spin-lock times of 4, 8, 16, 32, 12, 24, and 64 ms, respectively, were recorded consecutively. Because the C1−H1 correlations of all residues are within a small region (∼100−107 ppm), all signals of interest are well locked at the applied spin-lock strength of 3.141 kHz ($\theta > 80$). The values of the delays $\delta 1$ in the INEPT sequence (*33*) and $\delta 2$ in the sensitivity enhancement sequence were set to 1.56 ms

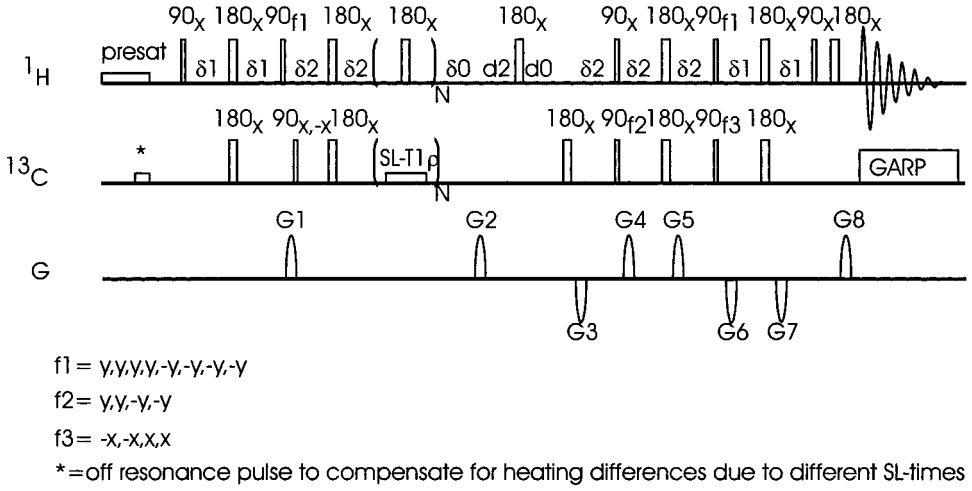

FIGURE 2: Pulse scheme of $T_{1\rho}$ measurements.

($1/4J_{C1-H1}$). The gradient strengths at the center of the sine-bell were as follows: G1 = 7.5, G2 = 0.75, G3 = −7.5, G4 = G5 = 0.0075, G6 = G7 = −0.0113, and G8 = 2.076 mT/cm. Spectra were recorded with 971 or 64 t_1 experiments and 88 or 336 scans of 1024 complex data points per increment for the line width or $T_{1\rho}$ spectra, respectively. Time-domain data were multiplied with squared-sine-bell functions shifted by $\pi/2$, which reduced truncation artifacts and did not influence relative peak integrals. Spectra with equal spin-lock times were added before integration of peaks. Integrals and $T_{1\rho}$ values were calculated using in-house software. Integrals were calculated using a radius of 11 Hz around the center of each peak. Data are fitted to the relation $I_z(\tau_m) = I_o \exp(-\tau_m/T_{1\rho}) + I_r$, where τ_m is the spin-lock time and I_r is the residual magnetization at long spin-lock times.

Processing of NMR Data Sets. NMR data sets were processed using Bruker UXNMR software or by means of the Triton NMR Software package (Bijvoet Center, Utrecht University). Resolution enhancement was achieved by multiplication of data with a phase-shifted squared-sine-bell window function, prior to zero-filling and Fourier transformation. The data sets were baseline corrected in each dimension by means of fifth-order polynomial fits.

RESULTS

Accessibility of the Glycans in αhCG in the Free Subunit versus the αβ-Heterodimer. Previously, it was demonstrated that of the two N-glycosylation sites Asn52 and Asn78 under native conditions only the glycan at Asn52 in αhCG is susceptible to cleavage by PNGase F. The specific and complete removal of the glycans at Asn52 (*34*) is depicted in the SDS−PAGE pattern in Figure 3 (compare lanes 1 and 2). To determine if this is typical for free αhCG, nondissociated hCG was treated with PNGase F using native conditions. As is evident from Figure 3, lanes 3 and 4, for intact hCG there is no change in the gel pattern after enzymatic treatment. This suggests that the impaired accessibility for PNGase F of the Asn52-linked glycan in hCG in comparison to free αhCG is due to association with the β-subunit.

Secondary and Tertiary Structure of Desialylated, Partially Deglycosylated αhCG. In the NMR spectra of αhCG, ^{1}H−

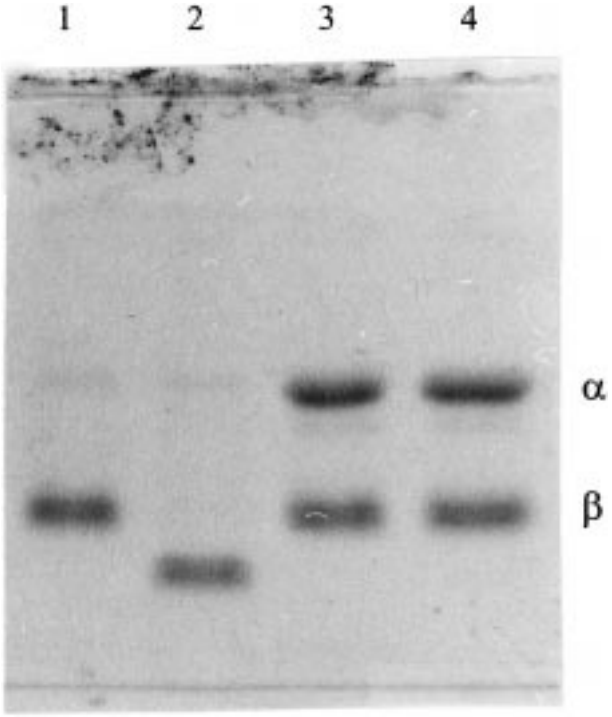

FIGURE 3: SDS−PAGE analysis. αhCG (lanes 1 and 2) and hCG (lanes 3 and 4) incubated with (lanes 2 and 4) or without PNGase F (lanes 1 and 3). The gel was stained with amido-black.

^{13}C correlations of Man-**3** and of the monosaccharide residues in the branches of the glycans at Asn52 and Asn78 overlap (*15*). To specifically observe the glycans at Asn78, those at Asn52 of αhCG were enzymatically removed (*34*). Because partial desialylation occurred at pH 5.1 at the temperatures used for NMR experiments, as was evident from two sets of signals for the galactose residues (*14*), the sample was completely desialylated in order to generate only terminal galactose residues. First, it was established whether it is justified to compare the structures of as-pdα and endo-B-treated αhCG carrying only the Asn-linked GlcNAc residues of which we previously achieved virtually complete resonance assignments (*15*). Spectra of as-pdα were cross-checked against the assignments for endo-B-treated αhCG by analyzing all spin systems and by identifying each NOE previously assigned. To compensate for the different tumbling rates (τ_c), the NOE mixing times used for the

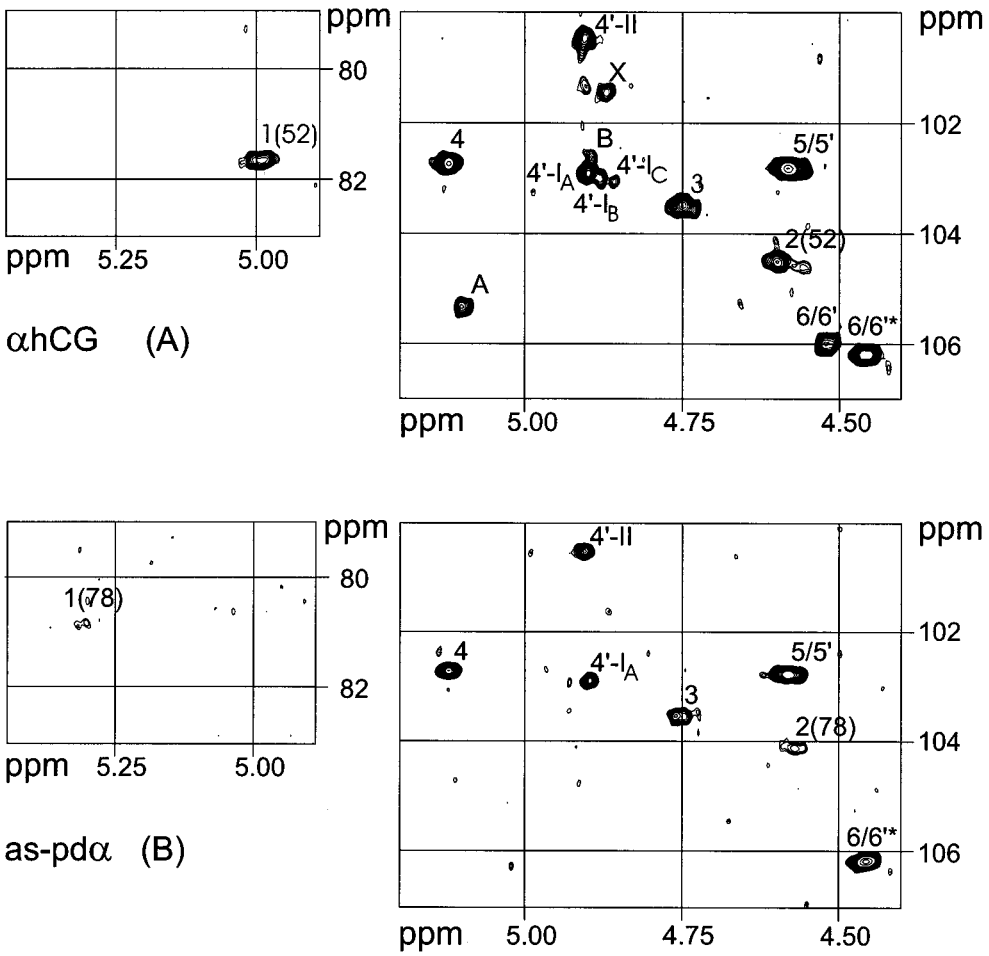

FIGURE 4: Parts of two-dimensional HSQC spectra. αhCG (A) and as-pdα (B) containing the carbohydrate anomeric ^{1}H−^{13}C correlations. Correlations are labeled with residue numbers: 4′-I_A corresponds to Man-**4**′ in the monoantennary structure, A, B, 4′-I_B, and 4′-I_C correspond to mannose residues in hybrid structures present at Asn52. X corresponds to GalNAc residues of the β-subunit of contaminating hCG (*15*).

spectra of as-pdα were shorter than for spectra of endo-B-treated αhCG. All amino acid residue signals are clearly broadened in the presence of glycosylation, and as a consequence, NOEs that are weak for endo-B-treated αhCG are often hardly or not observable in as-pdα spectra. Therefore, in the NOE spectra of as-pdα somewhat less NOEs were observed than in those of endo-B-treated αhCG. Nevertheless, for as-pdα the NOEs that were determined for the protein part indicated that the secondary structures of as-pdα and endo-B-treated αhCG are essentially alike. Also the contacts between the β-sheets were similar. In this way, almost all ^{1}H and many ^{13}C chemical shifts of the amino acids could be assigned (Supporting Information) and only minor differences in chemical shifts were found.

Next, ^{1}H and ^{13}C chemical shifts of the Asn78-linked glycan were determined for which advantage was taken of the data for the αhCG-bound N-linked glycans (*15*). In comparison to the earlier assignments for the intact α-subunit, some additional resonances could be identified, largely due to the elimination of overlap with the glycan at Asn52. The HSQC spectrum of as-pdα was recorded with less increments but with more scans per increment than used previously for the spectrum of intact α-subunit. The resulting increase in the signal/noise ratio allowed the novel assignment of the C1−H1 correlations of GlcNAc-**1** and GlcNAc-**2** (Figure 4). The other ^{1}H resonances of the GlcNAc-**2** residue, also not previously assigned, could be determined from the NH and NAcH tracks in TOCSY spectra. Thus, an almost complete assignment of ^{1}H and ^{13}C chemical shifts of the glycans attached to Asn78 was established (Table 1). The majority of the shifts of the glycans are virtually identical with those in the intact subunit (*15*). However, the NH signals of GlcNAc-**1**, -**5**, and -**5**′ have shifted 0.05 ppm upfield with respect to those reported previously. This may be a consequence of slight differences in sample conditions (e.g., pH, temperature, and salt). Comparison of the chemical shifts of GlcNAc-**2** with those determined for the GlcNAc-**2** residue of the glycan at Asn52 (*15*) shows that the chemical shifts of H4, H5, NAcH, and NH are significantly different, which is indicative of the proximity of the protein. The assignment of NOEs from GlcNAc-**1** H1 (δ 5.28) to the protein was hampered by the chemical shift overlap with Asn78 C$^\alpha$H (δ 5.28). The shift of the Asn78 C$^\alpha$H signal with respect to that of the corresponding proton in endo-B-treated αhCG suggests at least some structural change. Nevertheless, the overall NOE-pattern for GlcNAc-**1** to the protein was the same as in NOE-spectra of endo-B-treated αhCG, in which GlcNAc-**1** H1 (δ 5.28) and Asn78 C$^\alpha$H (δ 5.31) are well resolved (*15*).

Novel NOEs for the Glycan at Asn78. In αhCG, signals of glycans attached to Asn52 and Asn78 overlap. The advantage of the spectra of as-pdα is that we could now determine interresidual NOEs of the glycan at Asn78 (indicated in Figure 5). With the chemical shifts of

Table 1: Chemical Shifts of the Carbohydrates Attached to Asn78 in as-pdα

	chemical shift (ppm)[a]							
residue	H1 C1	H2 C2	H3 C3	H4 C4	H5 C5	H6a/H6b C6	NH	NAcH NAcC
GlcNAc-**1**	5.28	3.90	3.65	3.72	3.25	3.81/3.67	8.03	1.83
	80.9	nd	nd	nd	nd	63.0		25.8
GlcNAc-**2**	4.58	3.74	3.76*	3.73*	3.62	3.76/3.90*	8.00	1.98
	104.2	58.2[b]	nd	83.1*	nd	63.6*		25.5
Man-**3**(I)[c]	4.75	4.22	3.72	nd	3.60	nd		
	103.6*	nd	nd	nd	77.6	nd		
Man-**3**(II)[c]	4.77	4.23	3.76	3.81	3.63	3.75/3.90*		
	103.6	73.4	83.7	69.2	77.8	69.3*		
Man-**4**	5.13	4.18	3.90	3.53	3.75	3.64/3.89		
	102.7	80.0	72.8	70.8	76.8	65.0		
Man-**4'**(I)[c]	4.90	3.96	3.85	3.63	nd	nd		
	103.0	73.2	73.8	70.2	nd	nd		
Man-**4'**(II)[c]	4.91	4.09	3.86	3.52	nd	3.85/3.63*		
	100.6	79.9	72.9	70.8	nd	65.5*		
GlcNAc-**5**/GlcNAc-**5'**	4.60	3.73	3.71	3.70	3.57	3.86/3.97	7.96	2.04
	4.58	3.74	3.73	3.70	3.58	3.86/3.97	7.93	2.04
	102.8	58.2	75.3/75.4	82.2	78.1	63.5		25.7
Gal-**6**/**6'**	4.47	3.54	3.65	3.93	3.72	3.75*		
	106.2	74.3	76.0	71.9	78.6	64.0*		

[a] The ^{1}H chemical shifts are expressed by reference to internal acetone (δ_H 2.225). ^{13}C chemical shifts were referenced to the α-anomeric chemical shift of ^{13}C-labeled glucose (δ_C 94.8 versus 2,2-dimethyl-2-silapentane-5-sulfonic acid) at 328 K, pH 5.1. ^{13}C chemical shifts are assigned based on chemical shift data of αhCG (*15*). An asterisk (*) indicates tentative assignment. nd stands for not determined. [b] Indicates some overlap. [c] Type of glycan (Figure 5).

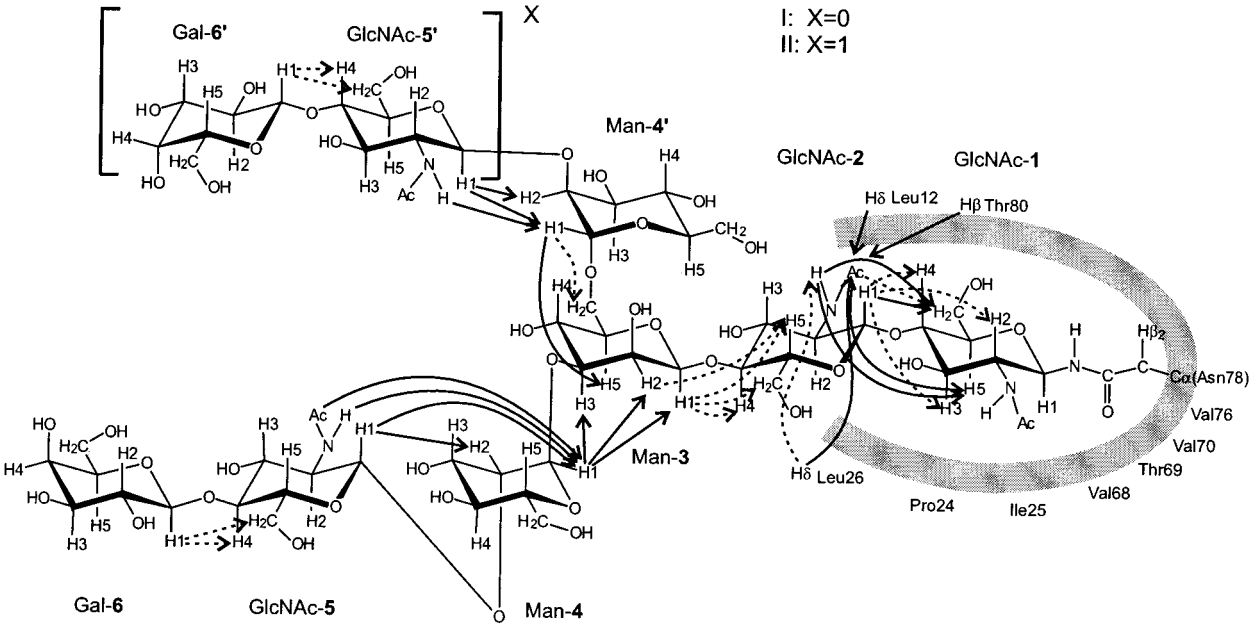

FIGURE 5: Glycan at Asn78. NOEs from GlcNAc-**1** to the protein are identical with those published previously (*15*) and not indicated in this figure. Intraresidual NOEs and NOEs from GlcNAc-**2** to protein are indicated with arrows. In case of overlap, arrows are dashed.

GlcNAc-**2** assigned, contacts to GlcNAc-**1** were determined that establish the orientation of these residues with respect to each other (see Figure 5). A difference between as-pdα and αhCG is the absence of the contact from H1 of Man-**4′** in the diantennary structure **(**II) to GlcNAc-**5′** NAcH (Figure 5), a contact which is clearly present in spectra of αhCG. This indicates that the orientation for the glycosidic linkage between Man-**4′**(II) and GlcNAc-**5′** is different from that in the glycan linked to Asn52. Also the contact from Man-**4** H2 to GlcNAc-**5** NAcH that was found in αhCG is absent in as-pdα. Thus, also the linkage between Man-**4** and GlcNAc-**5** may be changed. However, it cannot be excluded that this signal was of too low an intensity in the as-pdα spectrum because this NOE was weak in αhCG spectra wherein the signals of Man-**4** and GlcNAc-**5** of the glycans at Asn52 and Asn78 overlap.

Earlier in NOE spectra of αhCG, no NOEs between GlcNAc-**2** and amino acid residues were identified due to overlap. As a result of the reduction in overlap in the spectra of as-pdα, NOEs from GlcNAc-**2** NAcH to Leu12 C$^{\delta}$Hs, Leu26 C$^{\delta}$Hs, and Thr80 C$^{\delta}$Hs and from GlcNAc-**2** NH to Leu26 C$^{\delta}$Hs were now unambiguously assigned (indicated in Figure 5). Pro24 might be in the vicinity of GlcNAc-**2**, as can be deduced from NOEs from Pro24 to GlcNAc-**1** H3, H5, and H6 in endo-B-treated αhCG (*15*). However, resonances of C$^{\beta}$Hs and C$^{\gamma}$Hs of Pro24 could not be

determined for as-pdα since they are in a crowded region that has almost no resolution due to the broadened lines. No other NOEs between monosaccharide residues and the protein were observed, although it should be mentioned that most ring proton signals lie in a very crowded region and identification of NOEs within this region may be obscured due to overlap. The tracks of GlcNAc-**5** and GlcNAc-**5′** seem to be better resolved in spectra of as-pdα than in spectra of αhCG where signals for both the Asn52 and the Asn78 glycan are present. This could imply some difference in orientation or distance to the protein, but that could not be confirmed by any NOE.

Mobility of the Oligosaccharide at Asn78. Inspection of the part of the HSQC spectrum of as-pdα containing the C1−H1 correlations of the monosaccharide residues of the glycan at Asn78 (shown in Figure 4) reveals two previously not identified weak signals that are assigned to the anomeric ^{1}H−^{13}C cross-peaks of GlcNAc-**1** and GlcNAc-**2**. These assignments are based on the ^{1}H chemical shifts (assigned in homonuclear spectra) and on the ^{13}C chemical shifts being in the range of anomeric Glc ^{13}C chemical shifts. The intensities of these correlations are comparable to those of amino acid backbone $C^\alpha H-C^\alpha$ correlations in the structured and, hence, less mobile regions. Also the anomeric ^{1}H−^{13}C cross-peak of Man-**3** is weak, whereas for the other monosaccharide residues the C1−H1 correlations have high intensities (Figure 4). Comparison with the spectrum of αhCG shows that for αhCG only the GlcNAc-**2** signal stemming from the residue in the glycans attached to Asn52 is present. Thus, for the glycan at Asn52 all C1−H1 correlations are of about equal intensity, including those of the core residues. In the case of low mobility, line widths increase. To exactly determine the line widths of the C1−H1 correlations, a sensitivity-enhanced ^{1}H−^{13}C HSQC spectrum was recorded. The values of the delays in the INEPT sequence and in the sensitivity enhancement sequence were set to 1/4*J* for the (anomeric) CH meaning that CH_2 and CH_3 values are not sensitivity enhanced but a factor $\sqrt{2}$ is gained in intensity for the CHs. We applied these settings to record an HSQC spectrum on a sample of a relevant, free glycan (>10 mM) and indeed found an increase of signal/noise ratio. For as-pdα the experiment was optimized to have high resolution and signal/noise ratio in the carbohydrate C1−H1 region. Since the monosaccharide ring is considered to be relatively rigid as compared to the glycosidic linkages, the line widths of the C1−H1 correlations will represent the mobility of each constituting residue. The line widths and the corresponding T_2 values, which are directly derived from the line widths, are given in Table 2. For GlcNAc-**1**, no line width was determined because the signal/noise ratio was insufficient. Line widths for GlcNAc-**5** and -**5′** were not determined due to overlap, also for Gal-**6** and -**6′** no reliable results could be obtained because the signals are in too close proximity. The T_2 relaxation times increase for the residues further away from the protein, being especially pronounced from Man-**3** to the residues in the branches. Man-**4′** in the monoantennary structure (I in Figure 4) has a clearly longer T_2 relaxation time and thus a higher mobility than Man-**4**. This feature is expected since Man-**4′** (I) is a terminal residue, while interactions with the solvent of residues **5** and **6** reduce the mobility of Man-**4**. Man-**4** and Man-**4′** (II in Figure 4) have identical relaxation rates indicating that the (α1−3)- and the (α1−6)-linked branches have similar mobilities.

Table 2: Line Widths, Corresponding T_2 Values, and $T_{1\rho}$ Values of the Anomeric ^{13}C Nuclei of the Monosaccharide Residues in the Glycan at Asn78

residue	line width (Hz)[a]	T_2 (ms)[b]	$T_{1\rho}$ (ms)[c]	RMS
GlcNAc-**1**	>29	<11.7	<36	
GlcNAc-**2**	29	11.7 (9.8−14.5)	<36	
Man-**3**	20	17.5 (16.3−18.9)	36 ± 26	0.32
Man-**4**	7.2	59 (47−78)	78 ± 22	0.10
Man-**4′**(I)	6.1	74 (57−107)	107 ± 21	0.06
Man-**4′**(II)	7.2	59 (47−78)	79 ± 30	0.14
GlcNAc-**5/5′**	nd	nd	115 ± 20	0.05
Gal-**6/6′**	nd	nd	191 ± 20	0.02

[a] Resolution was 2.65 Hz/point. For GlcNAc-**2**, only the first 256 t_1 experiments were used because after these the signal had completely relaxed; therefore, the resolution was 10.6 Hz/point. The line width for Man-**3** may be overestimated due to a slight difference in chemical shift for Man-**3**(I) and Man-**3**(II). [b] T_2 values were calculated as follows; π*line width = $1/T_2$* with $1/T_2^* = 1/T_2 + 1/T_2^{B0}$. The line width of acetate (1.8 Hz) was used to ascertain $1/T_2^{B0}$ (5.65 Hz), the line broadening caused by the B0-field inhomogeneity, based on the assumption that for this small molecule $1/T_2 \ll 1/T_2^{B0}$. [c] The value for Man-**3** could be determined more accurately if 32 and 64 ms points were discarded and instead of integration with a radius of 11 Hz narrow boxes were used for integration; this gives a value of 28 ± 10 RMS = 0.11.

Since a quantification of the mobilities is not feasible at natural abundance with the present line widths, in addition $T_{1\rho}$ relaxation times of the anomeric carbon atoms were determined (Table 2). At the applied spin-lock strength all the observed signals are within the region of $\theta > 80$ and therefore $T_{1\rho} \rightarrow T_2$. The same conditions were used as for the spectrum recorded for the determination of line widths (see above). For GlcNAc-**1** and GlcNAc-**2**, no values could be determined due to their low intensity. GlcNAc-**5** and GlcNAc-**5′** signals overlap, and therefore they were integrated together. Analogously, integrals were determined of the combined Gal-**6** and Gal-**6′** signals. This is justified because the relaxation times are similar for the different branches as evidenced by the identical T_2 relaxation rates of Man-**4** and Man-**4′**(II). Furthermore, if the carbon atoms with overlapping signals relax at different rates, a summation is expected of two different exponential decays. As in both cases, the intensity of the combined signal steadily decays; this supports the assumption that the branches display similar mobilities. Man-**3** clearly has a shorter $T_{1\rho}$, and hence lower mobility than the residues in the branches. Man-**4** and Man-**4′**(II) have identical $T_{1\rho}$ relaxation rates. Thus, the $T_{1\rho}$ relaxation times display the same tendency as T_2 relaxation times. The observed increasing mobility for residues further away from the protein is extended to GlcNAc-**5**, GlcNAc-**5′**, Gal-**6**, and Gal-**6′** signals.

When comparing T_2 and $T_{1\rho}$ values, slightly higher values are found for $T_{1\rho}$. This can be explained as follows. In the $T_{1\rho}$ experiment, pure ^{13}C relaxation was measured along an effective field. In the HSQC experiment used for determination of T_2, the ^{13}C relaxation evolves as a combination of ^{13}C anti-phase magnetization and in-phase magnetization with respect to the attached proton. The C_xH_z magnetization generally relaxes considerably faster than the C_x magnetization, explaining the lower experimental values of T_2.

DISCUSSION

The present investigation was aimed at determining to which extent the mobility of the glycan at Asn78 of αhCG is restricted by the protein. To this end, a partially deglycosylated form of αhCG carrying only the glycan at Asn78 was used. Chemical shifts of the carbohydrate residues at Asn78 were assigned taking advantage of the elimination of overlap with the residues of the glycan at Asn52. The GlcNAc-**2** H4, H5, NAcH, and NH chemical shifts of this residue deviate noticeably from those of the corresponding residue at Asn52, indicating different chemical environments for these protons. Indeed, we established NOEs between NAcH, NH, and the protein and tentative contacts between H5 and Man-**3** H1 and H2. No such contacts were found in the case of the glycan at Asn52, although the contact to Man-**3** might be obscured by other overlapping signals. Furthermore, the overall NOE pattern for GlcNAc-**1** to the protein was the same as in NOE spectra of endo-B-treated αhCG (*15*). All other monosaccharide residues have chemical shifts similar to those in the free glycan, and no NOEs other than to neighboring monosaccharide residues were found, indicating that they are not in direct contact with the protein. Previously, we demonstrated that GlcNAc-**1** linked to Asn78 is an integral part of the hydrophobic core (*15*). The current results show that also GlcNAc-**2** is proximate to amino acid residues in the hydrophobic core, indicating that this residue is also involved in stabilizing the structure of αhCG. This is confirmed by the reduction of thermal stability of αhCG upon removal of the carbohydrate moiety beyond GlcNAc-**1** (*16*).

The initial observation that the $^{1}H-^{13}C$ correlation of GlcNAc-**1** at Asn78 had broadened beyond detection (*15*) was further investigated. Of all glycan residues, line widths and $T_{1\rho}$ relaxation times of the C1−H1 correlations were determined. A quantification of the mobilities would require that T_1 and T_2 relaxation rates of the protein backbone carbons are studied for determination of the overall tumbling rate. However, this was not feasible since the relaxation is extremely fast and ^{13}C measurements at natural abundance are inherently insensitive. Also, the protein is not globular. Nevertheless, our data give a picture of the motional behavior of this glycan. The values we found imply that the inner core residues of the glycan attached to Asn78 display mobilities that are similar to that of the protein, whereas the residues in the branches have a significantly higher mobility. Furthermore, it should be noted that all monosaccharide residues in the Asn52 glycan manifest strong $^{1}H-^{13}C$ correlations indicating high mobilities. Thus, the protein part of the α-subunit of hCG has a large influence on the dynamic behavior of the glycan at Asn78. Lommerse et al. (*13*) reported that monosaccharides display an accumulation of mobilities as they are further away from the glycosylation site even in the absence of interactions with the protein. Our previous studies on endo-B-treated αhCG demonstrated that Asn78 and Asn52 display broad and intense $^{1}H-^{13}C\ C^{\alpha}$ signals, respectively. Thus, the restricted mobility that is observed for the glycan at Asn78 is partially a consequence of the lower mobility at the attachment site and for another part attributable to specific interactions with the protein. Knowledge of the overall tumbling rate would be desirable to be able to separate these effects.

An interesting observation is that Man-**4** and Man-**4′**(II) display identical relaxational behavior, indicating similar mobilities for the (α1−3)- and the (α1−6)-linked branches. On one hand, the (α1−3)-linked branch will have some mobility as two different conformations have been suggested for the (α1−3)-glycosidic linkage (*35*). However, the (α1−6)-linked branch was expected to have a higher mobility than the (α1−3)-linked branch. First, the (α1−6)-linked branch of a free diantennary structure is known to have two major rotamer distributions around the Man-**3** C5−C6 bond in addition to the flexibility of the glycosidic linkage (*36*). Second, MD simulations have shown that in the free diantennary structure the dihedral angle ω [defined in the study of Rutherford and Homans (*37*) as H5−C5−C6−O6] of Man-**3**, and thus the orientation of the (α1−6)-linked branch, interconverts rapidly between 180° and −60° on the NMR time scale (*37*). Third, in a 21-amino acid glycopeptide, containing multiple glycoforms of N-linked diantennary oligosaccharides, the mobility of Man-**4′** is higher than that of Man-**4** (*38*). In the same study, it is proposed that the flexibility of the (α1−6)-linkage is caused by conformational exchanges on a relatively long time scale. Therefore, we suggest that the identical relaxation times of Man-**4** and Man-**4′**(II) mean that in the glycan at Asn78 the upper branch does not display this interconversion of ω and is restricted to either the extended or the backfolded conformation. Stubbs et al. (*39*) have demonstrated, using fluorescence energy transfer experiments on a diantennary N-glycan, that core fucosylation dramatically affects the conformation of the (α1−6)-linked antenna. In the present study, the contacts from the protein to GlcNAc-**1** and -**2** show that there is much steric hindrance around the inner core that may prevent backfolding, analogously to the effect of core fucosylation.

In this paper, it was shown that the PNGase F susceptibility of the Asn52-linked glycan of αhCG is abolished in nondissociated hCG, and the absence of susceptibility of the Asn78-linked glycan is retained. Also Weller et al. (*40*) studied the glycans of αhCG with and without dimerization with βhCG. They observed a disappearance of correlations from GlcNAc-**1** at Asn52 in heteronuclear NMR spectra upon dimerization, indicating reduction of mobility although this might solely be explained by an aspecific reduction in mobility of the glycan by the proximity of the slowly tumbling dimer. These results indicate that the high mobility of the glycan at Asn52 found in free αhCG cannot be extrapolated directly to the dimer. Also, this supports our model that folding of part of the α-subunit, containing Asn52, is dependent on the presence of the β-subunit (*15*).

In conclusion, NOEs, line widths, and $T_{1\rho}$ relaxation rates show that the mobility of the inner core of the glycan at Asn78 is greatly restricted by attachment to the protein. The mobility of the branches is high, although the relaxation rates of Man-**4** and Man-**4′**(II) indicate that compared to a free diantennary glycan for the (α1−6)-linked branch probably one rotamer distribution has become less favorable. It was demonstrated that not only GlcNAc-**1** but also GlcNAc-**2** has contacts to the protein that may lead to stabilization of the hydrophobic packing of the β-sheets, explaining the stabilizing effect of this glycan on αhCG. These results allow more accurate modeling of the glycan part of the intact glycoprotein, being a prerequisite for detailed investigations of the interaction with the receptor. Because the amino acid

sequence of the α-subunit and the inner core residues of the N-linked glycans of all glycoprotein hormones are identical, the effects of the glycan at Asn 78 will probably be the same in all these proteins. Our findings enlarge the view on how glycosylation contributes to the stability of proteins. This report adds to the general concept of the behavior of glycans that are covalently bound to a protein. Knowledge of this is essential for achieving an understanding of the total conformation of glycoproteins to model interactions with other biomolecules.

ACKNOWLEDGMENT

A crude preparation of hCG was kindly provided by Diosynth B.V., Oss, The Netherlands. We would like to thank Hans Vis and Frans Mulder for stimulating discussions. We are indebted to Johan Zwan, Hans Vis, and Frans Mulder for letting us use the in-house software.

SUPPORTING INFORMATION AVAILABLE

A table containing the ^{1}H and ^{13}C chemical shifts of the amino acids of as-pdα (αhCG desialylated and site-specifically deglycosylated at Asn52) (3 pages). Ordering information is given on any current masthead page.

REFERENCES

1. Sairam, M. R. (1989) *FASEB J. 3*, 1915−1926.
2. Iles, R. K., and Chard, T. (1993) *J. Mol. Endocrinol. 10*, 217−234.
3. Thotakura, N. R., and Blithe, D. L. (1995) *Glycobiology 5*, 3−10.
4. Matzuk, M. M., Keene, J. L., and Boime, I. (1989) *J. Biol. Chem. 264*, 2409−2414.
5. Matzuk, M. M., and Boime, I. (1988) *J. Cell Biol. 106*, 1049−1059.
6. Weisshaar, G., Hiyama, J., and Renwick, A. G. C. (1991) *Glycobiology 1*, 393−404.
7. Brockbank, R. L., and Vogel, H. J. (1990) *Biochemistry 29*, 5574−5583.
8. Wyss, D. F., Choi, J. S., and Wagner, G. (1995) *Biochemistry 34*, 1622−1634.
9. Wyss, D. F., Choi, J. S., Li, J., Knoppers, M. H., Willis, K. J., Arulanandam, A. R. N., Smolyar, A., Reinherz, E. L., and Wagner, G. (1995) *Science 269*, 1273−1278.
10. Fletcher, C. M., Harrison, R. A., Lachmann, P. J., and Neuhaus, D. (1994) *Structure 2*, 185−199.
11. Rutherford, T. J., Partridge, J., Weller, C. T., and Homans, S. W. (1993) *Biochemistry 32*, 12715−12724.
12. Lommerse, J. P. M., Kroon-Batenburg, L. M. J., Kamerling, J. P., and Vliegenthart, J. F. G. (1995) *Biochemistry 34*, 8196−8206.
13. Lommerse, J. P. M., Kroon-Batenburg, L. M. J., Kroon, J., Kamerling, J. P., and Vliegenthart, J. F. G. (1995) *J. Biomol. NMR 6*, 79−94.
14. De Beer, T., Van Zuylen, C. W. E. M., Hård, K., Boelens, R., Kaptein, R., Kamerling, J. P., and Vliegenthart, J. F. G. (1994) *FEBS Lett. 348*, 1−6.
15. De Beer, T., Van Zuylen, C. W. E. M., Leeflang, B. R., Hård, K., Boelens, R., Kaptein, R., Kamerling, J. P., and Vliegenthart, J. F. G. (1996) *Eur. J. Biochem. 241*, 229−242.
16. Van Zuylen, C. W. E. M., Kamerling, J. P., and Vliegenthart, J. F. G. (1997) *Biochem. Biophys. Res. Commun. 232*, 117−120.
17. Ryan, R. J., Charlesworth, M. C., McCormick, D. J., Milius, R. P., and Keutmann, H. T. (1988) *FASEB J. 2*, 2661−2669.
18. Vuister, G. W., Boelens, R., and Kaptein, R. (1988) *J. Magn. Reson. 80*, 176.
19. Piantini, U., Sørensen, O. W., and Ernst, R. R. (1982) *J. Am. Chem. Soc. 104*, 6800−6801.
20. Derome, A. E., and Williamson, M. P. (1990) *J. Magn. Reson. 88*, 177−185.
21. Braunschweiler, L., and Ernst, R. R. (1983) *J. Magn. Reson. 53*, 521−528.
22. Bax, A., and Davis, D. G. (1985) *J. Magn. Reson. 65*, 355−360.
23. Griesinger, C., Otting, G., Wüthrich, K., and Ernst, R. R. (1988) *J. Am. Chem. Soc. 110*, 7870−7872.
24. Jeener, J., Meier, B. H., Bachmann, P., and Ernst, R. R. (1979) *J. Chem. Phys. 71*, 4546−4553.
25. Bax, A., and Davis, D. G. (1985) *J. Magn. Reson. 63*, 207−213.
26. Bodenhausen, G., and Ruben, D. J. (1980) *Chem. Phys. Lett. 69*, 185−189.
27. Bax, A., and Pochapsky, S. S. (1992) *J. Magn. Reson. 99*, 638−643.
28. Marion, D., and Wüthrich, K. (1983) *Biochem. Biophys. Res. Commun. 113*, 967−974.
29. Marion, D., Ikura, M., Tschudin, R., and Bax, A. (1989) *J. Magn. Reson. 85*, 393−399.
30. Kay, L. E., Keifer, P., and Saarinen, T. (1992) *J. Am. Chem. Soc. 114*, 10663−10665.
31. Cavanagh, J., and Rance, M. (1993) *Annu. Rep. NMR Spectrosc. 27*, 1−58.
32. Peng, J. W., Thanabal, V., and Wagner, G. (1991) *J. Magn. Reson. 94*, 82−100.
33. Morris, G. A., and Freeman, R. (1979) *J. Am. Chem. Soc. 101*, 760−762.
34. Van Zuylen, C. W. E. M., de Beer, T., Rademaker, G. J., Haverkamp, J., Thomas-Oates, J. E., Hård, K., Kamerling, J. P., and Vliegenthart, J. F. G. (1995) *Eur. J. Biochem. 231*, 754−760.
35. De Waard, P., Leeflang, B. R., Vliegenthart, J. F. G., Boelens, R., Vuister, G. W., and Kaptein, R. (1992) *J. Biomol. NMR 2*, 211−226.
36. Brisson, J.-R., and Carver, J. P. (1983) *Biochemistry 22*, 3680−3686.
37. Rutherford, T. J., and Homans, S. W. (1994) *Biochemistry 33*, 9606−9614.
38. Lu, J., and Van Halbeek, H. (1997) *Biophys. J. 72*, 470−481.
39. Stubbs, H. J., Lih, J. J., Gustafson, T. L., and Rice, K. (1996) *Biochemistry 35*, 937−947.
40. Weller, C. T., Lustbader, J., Seshadri, K., Brown, J. M., Chadwick, C. A., Kolthoff, C. E., Ramnarain, S., Pollak, S., Canfield, R., and Homans, S. W. (1996) *Biochemistry 35*, 8815−8823.

BI9718548